UC San Diego
UC San Diego Previously Published Works

Title

Measurement of dissolved neon by isotope dilution using a quadrupole mass spectrometer

Permalink

Journal

ISSN

Authors

Hamme, Roberta C
Emerson, Steven R

Publication Date

2004-11-01

DOI

Peer reviewed

Measurement of dissolved neon by isotope dilution using a quadrupole mass spectrometer

Roberta C. Hamme[*]

Scripps Institution of Oceanography, University of California San Diego,
9500 Gilman Drive, Dept 0244, La Jolla, CA 92093-0244, USA

Steven R. Emerson

School of Oceanography, University of Washington,
Box 355351, Seattle, WA 98195-5351, USA

Abstract

We describe an analytical method with improved precision for measuring the concentration of neon dissolved in water. Measurements were calibrated by isotope dilution, with addition of a ^{22}Ne spike directly to the evacuated sample flask prior to water collection. The use of glass flasks for water sampling, with flushing of air from the system by CO_2, greatly reduced the chance of contamination. Dissolved gases were extracted from the water sample by equilibration with a headspace and cryogenically processed to remove interferences. The ^{22}Ne/^{20}Ne ratio was then measured on a quadrupole mass spectrometer operated in static mode. Mass fractionation by the system was accounted for by frequent analyses of the ^{22}Ne/^{20}Ne ratio in air. We routinely obtained precisions of ±0.13% based on the standard deviation of duplicate field samples. Accuracy of the method, in the form of possible systematic offsets that could skew all the data, was assessed to be ±0.18%, excluding a possible ±0.2% error in the estimate of the Ne concentration of air.

1 Introduction

Observed concentrations of neon dissolved in seawater are greater than would be expected for equilibrium with the atmosphere. The supersaturation of Ne is generally controlled by a balance of diffusive and bubble-mediated gas exchange, temperature change, and atmospheric pressure deviations (Jenkins, 1988; Hamme and Emerson, 2002; Well and Roether, 2003). In some regions, ice processes also play an important role (Hohmann et al., 2002). Neon is less soluble than many inert gases and therefore has been recognized as a sensitive tracer of bubble dissolution caused by breaking waves (Bieri, 1971; Craig and Weiss, 1971). As a tracer, Ne is also useful because its solubility curve is less dependent on temperature than gases like Ar and N_2 are. These unique physical properties mean that accurate and precise measurements of Ne, in combination with other gases, allow rates of gas exchange and temperature change to be quantified.

Beyond improving estimates of bubble-mediated gas exchange, better Ne measurements will help to reduce uncertainties in a number of specific applications. Carbon export can be determined from an oxygen mass balance, but only if the effect of bubbles on oxygen supersaturations can be accurately estimated from measurement of gases like Ne (Craig and Hayward, 1987; Spitzer and Jenkins, 1989; Emerson et al., 1995; Hamme, 2003).

---

[*]Corresponding author. Tel.: +1-858-822-5946; Fax: +1-858-822-3310; E-mail: rhamme@ucsd.edu

Table 1: Comparison of published Ne analysis methods and their precisions

Reference	Purification method	Standardization method	Precision (%)
This work	77K charcoal trap	isotope dilution	0.13
Kulongoski and Hilton (2002)	getter & 77K charcoal trap	isotope dilution	0.7
Lott (2001)	getter & 9K stainless trap	air aliquots	0.3
Hood (1998)	getter & 8K charcoal trap	air aliquots	0.3
Roether et al. (1998)	25K charcoal trap	air aliquots	0.4
Ludin et al. (1998)	24K and 10K charcoal traps	air aliquots	0.2–0.5
Poole et al. (1997)	getter & 77K charcoal trap	isotope dilution	0.3
Top et al. (1988)	77K charcoal trap	isotope dilution	< 1
Sano et al. (1982)	combustion & 77K charcoal trap	air aliquots	10-20
Bieri et al. (1968)	getter & 77K charcoal trap	isotope dilution	0.6–1.5
Craig et al. (1967)	getter & 77K charcoal trap	isotope dilution	1.4

Clues to water mass ventilation can be obtained from flux estimates of ^{3}He at the surface, and Ne data are commonly used to correct ^{3}He for the presence of injected air (Jenkins, 1988). Moreover, dissolved Ne concentrations can be used to determine paleotemperatures from ground waters (Stute et al., 1992; Stute and Schlosser, 1993), to estimate glacial meltwater fluxes (Hohmann et al., 2002), and to calculate the fraction of helium released from the earth's mantle and crust (Craig and Weiss, 1971; Roether et al., 1998, 2001).

Water samples for Ne analysis are usually collected in copper tubes by flowing water through the tube and then crimping the ends (Weiss, 1968). When properly used, copper tubes provide excellent sample preservation (Spitzer, 1989). For analysis, copper tubes are attached to a vacuum line where the dissolved gases are fully extracted from the water (Hood, 1998; Ludin et al., 1998). The most common method of quantifying Ne samples is quadrupole mass spectrometry in static mode, but methods used to separate Ne from interfering gases and to standardize the measurement differ (Table 1). Often, reactive gases are first removed by absorption onto a gettering material or by combustion. The heavier noble gases are then absorbed on to activated charcoal or stainless steel held at liquid N_2 temperatures or less (Lott and Jenkins, 1984; Lott, 2001), leaving Ne and He free to enter the mass spectrometer. Methods of standardization are either by comparison with separate analyses of air aliquots or by isotope dilution.

The most important potential source of error in these methods is the accidental trapping of air bubbles in the copper tubes during sampling. Because Ne is so insoluble, a very small amount of air can overwhelm the dissolved signal. Clear signs of air contamination were detected by Well and Roether (2003) in 5-20% of Ne samples collected on multiple cruises in the South Atlantic and South Pacific from 1990 to 1999, while further samples may have been more subtly affected. Drift between analysis of standards and samples and incomplete extraction of neon from the water may also lower precision for some methods.

The goal of this paper is to fully describe an accurate and precise method for the measurement of dissolved Ne by isotope dilution using a quadrupole mass spectrometer. This method uses a different technique for water sample collection to reduce the possibility of air contamination, although some new difficulties with sample preservation are introduced. Isotope dilution removes the necessity to completely extract gas from the water and controls for drift in the sensitivity of the mass spectrometer. A precision of $\pm$ 0.13%, based on duplicate field samples, demonstrates the worth of these method improvements. We assessed the accuracy of this method at $\pm0.18\%$, excluding error in the known Ne concentration of air, which cancels when saturations are calculated, and $\pm$ 0.27% including this error.
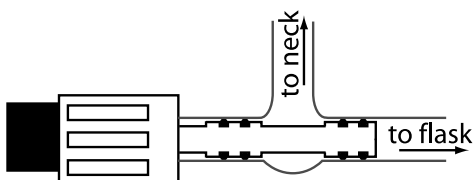
Figure 1: Schematic of the custom Louwers-Hapert O-ring sealing valves used on our glass sample flasks. The standard plunger was extended by 5 mm so that a second O-ring could be added to the sealing end.

2 Analytical method

2.1 Isotope dilution and purification

Pure ^{22}Ne (Isotec, isotopic enrichment $\geq$ 99.9%) was diluted with N_2 to a concentration of approximately 11 ppm Ne and stored in a 5-l glass reservoir with a 2-mL aliquoting valve. Aliquots of the diluted spike were added to evacuated 160-mL cylindrical glass sampling flasks, fitted with custom Louwers-Hapert 9-mm glass valves with dual O-rings on the sealing end of the plunger (Figure 1). The spike addition was performed in a small glass vacuum line inside a temperature-stabilized box (Figure 2). The pressure of the spike in the sample flask and vacuum line was measured just as the first sealing O-ring on the sample flask was engaged. This pressure was approximately 600 Pa (4.5 Torr) and was measured to a precision of $\pm$ 0.1 Pa (0.001 Torr) on an MKS Baratron 10-Torr pressure gauge (model 122AA-00010AD with an accuracy of $\pm$ 0.15%). The gauge's zero reading was determined prior to each spike addition to correct for changes in zero stability (Hyland and Tilford, 1985). Temperature was measured to a precision of $\pm$ 0.02 °C on a mercury thermometer inside the box. Previous to the spike addition, sample flask volumes were determined to a precision of $\pm$ 0.06 ml by comparing the masses of the flasks when evacuated and when filled with water of a known temperature. Using the ideal gas law (PV=nRT), we then calculated the moles of ^{22}Ne spike added to each sample flask based only on the concentration of the spike, the measured pressure of the spike during addition, the volume of the flask, and the temperature inside the box.

The concentration of the spike was determined multi-ple times by reverse isotope dilution with air. Spike was added to one sample flask and a known pressure of air to another. The two flasks were connected with a Cajon Ultra-Torr Tee and allowed to mix together for 1 h, while one flask was heated to encourage convection. The ^{22}Ne/^{20}Ne ratio was then measured on both flasks, and the concentration of the spike calculated from the known concentration of 18.18ppm Ne in air (Glueckauf, 1951). No difference was found between spike calibrations using air collected outside the building and using dry, commercially prepared, low hydrocarbon air.

2.2 Sampling

After adding the spike, the necks of the sample flasks were filled with CO_2 and sealed with tight-fitting plastic caps, to reduce contamination by air leakage across the O-rings. Because changing air pressure during transport must force air past the plastic cap, the flask necks were again flushed with CO_2 and sealed after arrival at the sampling location. On long cruises, the flask necks were kept evacuated by a vacuum pump to a pressure of less than a few tenths of a pascal (a few mTorr) using a custom-made stainless steel manifold with 3/8" Ultra-Torr adapters.

To collect the water sample, the neck of the flask and the space between the dual O-rings was first flushed with fresh CO_2. A thin line flowing seawater directly from a Niskin bottle was inserted into the neck of the flask as the CO_2 line was removed. The valve was tapped to remove excess bubbles as seawater continued to flush the neck. Then, the valve was very slightly cracked open, and seawater was sucked into the flask until it was about half full [see Emerson et al. (1999) for full sample collection details]. This sampling procedure prevented the accidental introduction of air bubbles to the sample, because only very small CO_2 bubbles could be present when water was allowed into the flask. In addition, the large gradient in pressure between the water flushing the neck and the near vacuum in the flask prevented any spike from leaking out at this stage.

After sampling, the necks and the space between the dual O-rings were carefully cleaned with fresh water and dried using a vacuum pump. On long cruises, flasks were reconnected to the vacuum manifold at this time. Otherwise, a vacuum was left between the dual O-rings, and
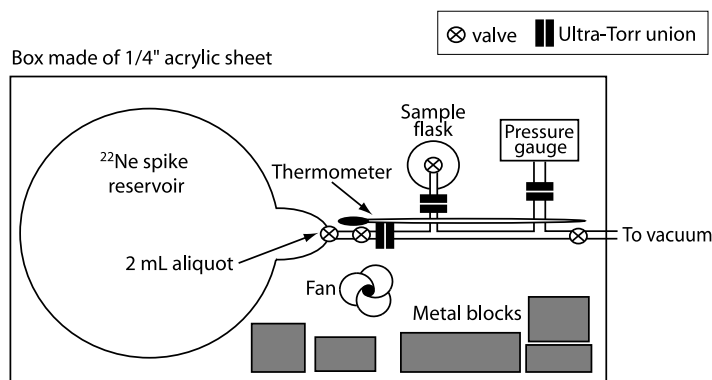
Figure 2: Schematic of the system used to add an aliquot of ^{22}Ne spike to a sample flask. All valves were glass Louwers-Hapert O-ring sealing valves and extended through the front wall of the box. The 2-ml aliquoting valve was made from a two-way Louwers-Hapert glass valve. The exact volume and reproducibility of this aliquoting valve did not affect the spike addition procedure. Metal blocks on the bottom of the box provided thermal inertia to the system. A fan, attached to the back wall, circulated the air inside the box. The top of the box was removable.

CO_2 was placed in the necks for transport back to the laboratory.

2.3 Sample processing

After sample flasks were returned from the field, they were weighed to a precision of $\pm$ 0.01 g. Although most of the dissolved gas rushed into the headspace during sampling, it was important to achieve equilibrium between the two phases. To this end, flasks were placed on a slowly rotating rack immersed in a constant temperature water bath for at least 8 h at $\sim$22 ^{o}C. Previous experiments with $O_2/N_2/Ar$ ratios have shown that 8 h is sufficient to reach equilibrium for these gases (Emerson et al., 1999). Because Ne diffuses faster, it must also reach equilibrium in this amount of time. Based on its solubility, greater than 99% of the Ne in the original water sample was present in the headspace after equilibration. Upon removal from the bath, sample flasks were inverted, taking care to prevent bubble formation, and attached to a vacuum flask. The water sample was then removed by suction until <1 ml remained, leaving the gas phase fully intact. Finally, the flask necks and space between the dual O-rings were cleaned, and the flask necks attached to a manifold evacuated by a vacuum pump until analysis.

In preparation for the analysis, each sample was cryogenically purified on a glass vacuum line directly connected to the quadrupole mass spectrometer used for the measurement (QMS) (Figure 3). A sample flask was attached to the line with an Ultra-Torr union, and then immersed in liquid N_2. The line was evacuated for approximately 30 min to a pressure of less than 0.1 Pa (1 mTorr), with an oil diffusion pump backed by a rotary rough pump. After isolating the line from the vacuum pump, the flask was opened and the sample allowed to flow sequentially through two liquid N_2 traps, for 1 min each, to remove H_2O and CO_2. The sample then proceeded to a U trap packed with activated charcoal also immersed in liquid N_2. Over the course of 15 minutes the major gases (N_2, O_2, Ar) in the sample absorbed onto the charcoal surface, leaving only Ne and He in the processing line. The line was then directly opened to the QMS, allowing the sample to enter the mass spectrometer. The pressure in the line did not rise above 0.1 Pa (1 mTorr) during the analysis, although blanks showed that a small amount of air did diffuse into the processing line while it was isolated from the vacuum.
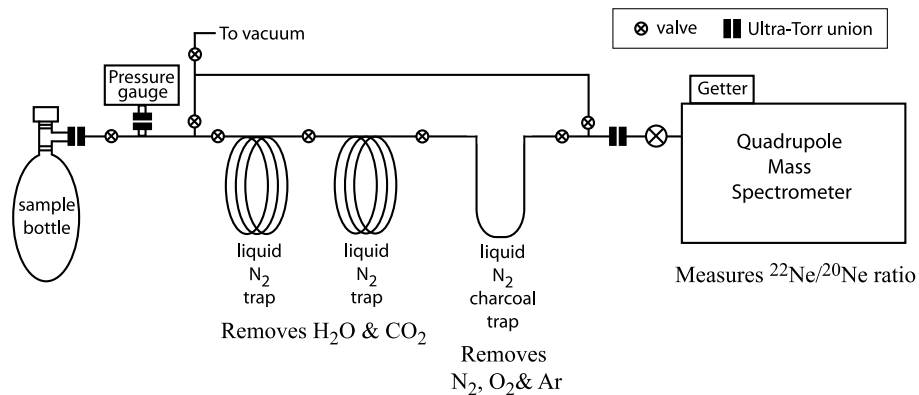
Figure 3: Schematic of the cryogenic vacuum line used to remove interfering gases from the Ne sample before analysis in the QMS. All lines were made from 3/8" glass tubing except the charcoal trap which was 1/2" glass tubing and the last section of the line connected directly to the QMS which was stainless steel. Valves were all glass Louwers-Hapert 9-mm valves except the last valve before the QMS, which was a Nupro stainless steel valve. The pressure gauge was a 10-Torr MKS Baratron.

2.4 QMS analysis

The ratio of masses 22 to 20 in the sample was determined using a UTI 100C quadrupole mass spectrometer with a Channeltron continuous dynode electron multiplier detector and an open source utilizing yttrium-oxide-coated iridium filaments. Samples were run in static mode, meaning that the spectrometer was isolated from the vacuum system. This increased signal strength to acceptable levels and allowed the sample ratio to be measured for a long period of time. The QMS repeatedly swept from mass 17 to 23 every 12 s. Its 0- to 10- V analog output signal was converted to digital with a 12-bit A/D converter and stored at 16-msec intervals. The scan rate was set to 12 s so that at least 100 points per peak were stored. A faster data conversion and storage rate would have allowed faster scans and is a suggested improvement to reduce sample analysis time. Each sample was observed for approximately an hour, generating ~200 measurements after the ratio reached a plateau. The total analysis time was chosen to reduce the standard deviation of the mean of the ratio to approximately 0.03%. Changing the analysis time within reasonable constraints did not affect the final ratio.

The QMS signal baseline was measured at mass 23, because the small ^{21}Ne peak prevented the signal from completely returning to baseline between the larger peaks at masses 20 and 22. Random Gaussian noise of unknown source was present in the output signal at a constant level of $0.5\text{-}1*10^{-11}$ amps at typical sample amplifications, compared with peak heights in the $1\text{-}9*10^{-9}$ amps range. The QMS electronics can perform some noise dampening, but concerns that further dampening would distort the peak shapes forced us to allow this level of noise to remain in the signal. It was also tempting to integrate the peak areas to obtain the ^{22}Ne/^{20}Ne ratio in order to reduce the effect of the noise. However, the lack of full peak separation between the three Ne isotopes, as well as variability in peak width over time, meant that only peak heights were acceptable for this application.

Our MatLab algorithm to determine peak height was carefully designed to avoid two possible sources of bias. First, because the peaks were slightly different widths, extensive filtering to remove noise would have introduced a bias to the ratio. Second, to avoid biasing by the presence of noise in the signal, it is important to evaluate the peak height at the same location on each peak in every scan, so that random noise will cancel. We found that noise in the signal was large enough to cause the maximum peak height to randomly shift location near the top of the peak. This was especially problematic for two peaks of differ-

ent sizes, because the smaller peak will be more biased by a constant noise level. The procedure we settled on began by filtering the peaks with an 80-point running mean, which was just a bit less than the distance between the peak top of one peak and the tail of the other. Information from the filtered peaks was then used to determine a consistent location on the unfiltered peaks for the maximum peak height. A mean of the four points nearest this maximum peak height location on each unfiltered peak determined the ^{22}Ne/^{20}Ne ratio for each scan.

3   Results and Discussion

3.1   Sample preservation tests

Preventing air from leaking past the Viton O-rings and into the glass flasks was important to the success of the sampling method. Preservation experiments were performed by filling the necks of evacuated flasks with different substances and sealing them with tight-fitting plastic caps. After waiting a set number of days, the Ne content of the flasks was determined on the QMS and compared to the expected content of a typical water sample (Table 2). In general, the leak rate for flasks with the custom dual O-ring stopcocks (Figure 1) was two to three times less than for those with standard single O-ring stopcocks. The small volume between the two O-rings, $\sim$0.1 ml, theoretically prevents the dual O-ring stopcocks from performing better than this. Continuous evacuation of the flask necks by a vacuum pump until analysis was the best preservation method. This technique reduced the leak to 0.1% or less of the expected content of a typical water sample, even over 50 days. Filling the flask necks with CO_2 was the next most effective at reducing leaks around the O-rings, followed by degassed water, regular water, and finally air. A special technique for sealing in which the cap was also flushed with CO_2 as it was placed on the neck further reduced the leak rate by trapping less air in the neck. A short series of preservation experiments using flasks containing the usual amount of spike indicated that the leak rate was lower when spike was present in the flask than when it was evacuated. The results for preservation with water were surprising, because the reduced diffusion rate of gases in water might be expected to slow leak rates considerably. It may be difficult to completely remove

Table 2: Summary of sample preservation tests.

Substance in neck	# O-rings	# Days	# Replicates	% Of sample
Vacuum	1	7–8	3	<0.1
Vacuum	1	16–52	5	0.1
CO_2	2	7	1	0.1
CO_2	1	7	3	0.2
CO_2	2	15–22	5	0.2
CO_2	1	20–21	4	0.5
CO_2*	1	20–21	4	1.2
Degassed water	2	7	1	0.7
Degassed water	1	7	2	0.5
Water	2	10–15	2	0.8
Water	1	9–14	2	1.8
Air	2	8	1	1.0
Air	1	8	1	3.1

The last column indicates the average amount of ^{20}Ne that leaked into the flask in terms of the percent impact on a typical water sample.
* indicates no special cap technique.

tiny air bubbles from the O-ring by flushing the neck with water, or an air bubble may be more easily trapped under the cap when filling with water as opposed to CO_2.

Based on these results, only flasks with dual O-ring stopcocks were used for Ne samples. Flasks containing water samples or just the ^{22}Ne spike were allowed to sit for up to 10 days with CO_2 in the necks. On longer cruises and at all times in the laboratory, flasks were attached to a vacuum manifold so that the necks were kept evacuated by a rough pump to a pressure of less than a few tenths of a pascal (a few mTorr). Our preservation tests, performed on evacuated flasks, suggest that leaks may raise the Ne concentration of the sample by as much as 0.1% for these conditions. However, the presence of the spike or water in the flask changes the gradient across the O-rings, and experiments show that this reduces the leak rate. During vacuum preservation prior to admitting a water sample into the flask, there is little risk of significant amounts of spike leaking out of the flasks. This is because the gradient from the Ne in the flask to a vacuum is 250 times less than that from air to a vacuum, due to the low pressure of the spike inside the flask. Flasks containing only spike would have to remain on the vacuum manifold for

at least 50 days before the leak could affect our analysis by 0.2%. After sampling, there is even less concern of leakage out of the flask, because the ratio of the two Ne isotopes is then close to one. A modeling exercise based on our preservation tests suggested that fractionation would have a negligible effect on the ^{22}Ne/^{20}Ne ratio during vacuum preservation of water samples.

3.2 Analysis Issues

Each sample run had to be corrected for the time-dependent blank at masses 20 and 22. During purification and analysis of the samples, a small amount of Ne diffused into the cryogenic processing line, which was isolated from the vacuum. Leaks through the Cajon Ultra-Torr compression fittings [fluorocarbon elastomer (FKM) O-rings] accounted for the majority of the blank, and we were able to halve the blank by removing three unnecessary Ultra-Torr fittings from the line. Blanks were assessed about twice a month by evacuating a flask and running it like a normal sample. Typically, the signal measured at mass 20 for a blank was 0.1-0.2% of the signal expected for a water sample (Figure 4), while the blank at mass 22 was about five times smaller. The blank increased over the course of the entire run as Ne continued to diffuse into the processing line. The average mass 20 blank observed at 40 min was $4.3 \pm 0.8*10^{-12}$ amps, with some of this variability caused by long-term drifts in the sensitivity of the mass spectrometer rather than random fluctuations.

If just air was leaking into the processing line, the blank measured at mass 22 would be expected to be about 10 times less than at mass 20. That this was not the case may indicate a small memory effect due to the O-rings absorbing Ne in a 1:1 isotopic ratio from the samples. If a memory effect was indeed responsible, it was very constant because blanks run at the beginning of the day did not differ from those run interspersed with samples.

During analysis, measurable amounts of H_2, He, H_2O, CO, Ar, and CO_2 were present in the QMS. By isolating the QMS from both the vacuum and sample processing line, we determined that H_2, H_2O, CO, and CO_2 were degassing from the filaments and metal walls inside the QMS. Water also entered the QMS during analysis from the cryogenic processing line. Of these reactive species, H_2O and CO_2 were a concern because $H_2^{18}O$ has a mass
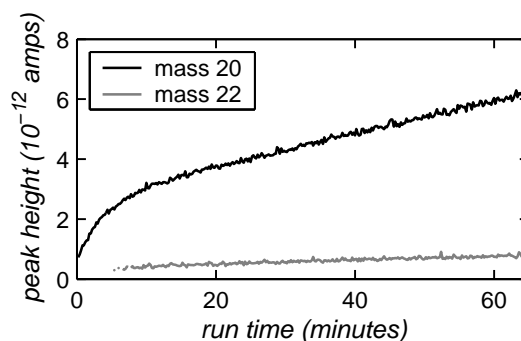

Figure 4: Example of typical blank run showing the current measured at the maximum peak height for masses 20 and 22. Run time indicates the time since the valve between the processing line and the QMS was opened. For comparison, the peak heights for water sample analyses were approximately $3*10^{-9}$ amps at both masses.

of 20, which interferes with the measurement of ^{20}Ne, and doubly charged CO_2 has a mass to charge ratio of 22, which interferes with the measurement of ^{22}Ne. To reduce H_2O contamination, the processing line was actively evacuated with the rough pump when not in use, and the last section of the line was heated between samples to drive off moisture adhering to the glass. Inside the QMS, we installed a small getter (SAES Getters Metal Appendage Pump with St 707 Zr-V-Fe getter material) to absorb the reactive species: H_2, H_2O, CO and CO_2. Finally, the ionizer electron energy was decreased from 70 to 35 V to reduce the amount of doubly charged CO_2 produced during ionization. These steps reduced the H_2O signal at mass 18 to less than $1*10^{-11}$ amps, and the CO_2 signal at mass 44 to about $3*10^{-10}$ amps, compared with ^{20}Ne and ^{22}Ne signals of $3*10^{-9}$ amps for a typical water sample. At these levels of contamination, H_2O and CO_2 only affected the Ne measurement at a level of about 0.001%.

Of the nonreactive species present in the QMS, only Ar presented a possible problem, because doubly charged Ar has a mass to charge ratio of 20, which interferes with the measurement of ^{20}Ne. The charcoal trap could not completely absorb all the Ar in a sample and the tiny amount of free Ar caused a signal of about $1*10^{-10}$ amps at
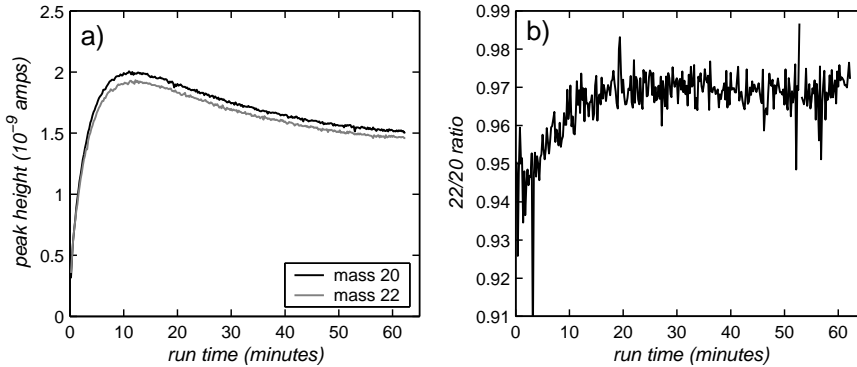
Figure 5: (a) Example of the current measured at the maximum peak height for masses 20 and 22 over the course of a typical water sample analysis. (b) The blank-corrected $^{22}Ne/^{20}Ne$ ratio for the same sample.

mass 40. Because the ionization conditions were tailored to reduce double ionization, the contribution of doubly-charged Ar to the current at mass 20 was less than 0.01%. We estimated the contribution from doubly charged ions, by allowing a larger quantity of Ar or CO_2 (before the getter was installed) into the QMS and measuring the effect on the signals at masses 20 or 22.

Ions with lower mass to charge ratios produce a greater response by the electron multiplier detector, resulting in mass fractionation in the measurement of the two Ne isotopes. We characterized this process by measuring the $^{22}Ne/^{20}Ne$ ratio of air samples to determine a mass fractionation factor (MFF). For each MFF analysis, a sample flask was first filled with air collected outside the building. The sample size was reduced to about 2% of the original air sample, by expanding the sample into larger volumes and then evacuating them, in order to more closely match the pressure of the water samples. The reduced air sample was then cryogenically processed and analyzed in the same way as a water sample. The measured $^{22}Ne/^{20}Ne$ ratio was compared to the actual ratio in air, 0.1020 (Eberhardt et al., 1965; Walton and Cameron, 1966) to determine the MFF (defined here as the actual ratio / measured ratio). The MFF was evaluated every day that samples were analysed and was found to vary from 1.08 to 1.10, changing slowly over a time scale of months. An MFF of 1.05 is predicted for $^{22}Ne/^{20}Ne$ with this type of electron multiplier (MKS Instruments, 1998). The frequent measurement of essentially identical air samples also proved

to be a useful diagnostic tool in detecting subtle electronics problems, such as isolated capacitor and resistor failures in the QMS signal-processing components.

Although the $^{22}Ne/^{20}Ne$ ratio stabilized after about 20 min, the individual signals at masses 20 and 22 did not reach a stable plateau (Figure 5). Calculation of the mean free path in the cryogenic processing line after the major gases had been absorbed onto the charcoal trap suggested that the transport of Ne into the QMS was controlled by molecular diffusion. The increase in the individual signals during the first 10 min must have been caused by the slow diffusion of gases into the QMS, especially through the inline trap packed with activated charcoal granules, which would have acted as a significant barrier to diffusion. Because ^{20}Ne diffuses faster than ^{22}Ne, diffusional control also explains why the $^{22}Ne/^{20}Ne$ ratio was initially lower than the final value. Ion consumption, a process by which ions moving down the mass filter are buried in the walls of the QMS, was probably the cause of the subsequent signal decrease over time, and is a common feature of static quadrupole mass spectrometry (Rau and Putzka, 1999). The buried ions did not seem to cause a memory effect, as evidenced by the similarity between blanks run at the beginning of the day and those run after samples, and also by the absence of an increase in Ne when the QMS was isolated from both the vacuum and processing line.

The ^{20}Ne and ^{22}Ne peak shapes were identical, but had some fine structure and were not symmetrical (Figure 6).
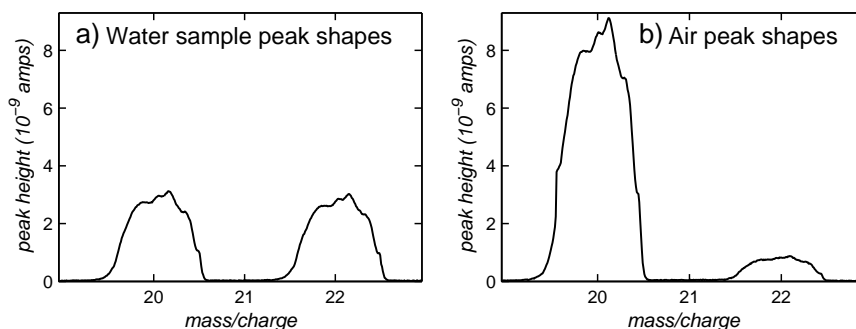
Figure 6: (a) Example of the current measured over the 19–23 mass range showing the peak shapes and relative sizes for a typical water sample run. (b) Same as (a) but for a typical air run. The ^{21}Ne peak is too small to observe on this scale.

The same structure was also observed at other masses. We qualitatively optimized the emission current, ion energy, and focus voltage to obtain the best peak shape possible while maintaining acceptable sensitivity. This optimization affected the size of the bumps and the peaks themselves, but not the position of the bumps on the peak. The specific location of the bumps is probably specific to each ionizer (Marty Suorsa, personal communication). While the peak shape was not ideal, it was extremely reproducible on monthly timescales and certainly over the course of a single run. The reproducibility of the peak shapes allowed ratios to be calculated from peak heights. Otherwise, precision could not have been maintained.

The electron multiplier gain slowly varied by 10-20% over the course of several years, but this had no effect on the sample accuracy because of the use of isotope dilution. At high sample pressures, nonlinear effects and severely distorted peak shapes can be a problem, hence pressures inside the QMS were always kept several orders of magnitude below the maximum operating pressure of 1.3 mPa (10^{-5} Torr) for this type of ionization source (MKS Instruments, 1998). In a typical water sample, the combined pressure of all the contaminant ions in the QMS was similar to that of each Ne isotope. No relationship was observed between the mass of the water sample, which should be related to the total pressure of Ne, and deviations in the measured ratio. From this, we conclude that changes in the pressure inside the QMS from sample to sample did not affect the discrimination between masses.

3.3   Error Analysis

Ne concentrations determined on 170 pairs of duplicate field samples, collected from 2000 through 2002, had a mean relative standard deviation of 0.13 ± 0.10 %. This estimate of the precision includes errors resulting from variability in flask preparation, sampling, preservation, blank variability, processing, and analysis. The precision of just the ^{22}Ne/^{20}Ne ratio determined by the QMS was $\pm 0.03\%$ (relative standard deviation of the mean). Precision can also be estimated by comparing deep water samples collected in the same location. We calculated a mean precision of $\pm 0.20\%$ using samples from 1000, 2000, 3000, 4000, and 4600 m (15–21 samples per depth) collected at Station Aloha, Hawaii Ocean Time-series (HOT), on 11 cruises between July 2000 and June 2001. Ne saturations in the deep North Pacific should not display significant natural variability on an annual basis. The larger error estimated by this deep sample comparison indicates that the method was affected by some type of monthly timescale variability. The most likely source of this variability was either failure to completely account for changes in the mass fractionation factor (MFF) or drift in the calibration of the pressure gauge used to add the spike.

Determining the ^{22}Ne/^{20}Ne ratio of air samples, in order to evaluate mass fractionation, was more difficult than for the spiked water samples. The amount of spike added to the flasks was specifically targeted to make the final ^{22}Ne/^{20}Ne ratio of the water samples near one. How-

9

ever, for air samples, the ^{22}Ne peak was nearly 10 times smaller than the ^{20}Ne peak (Figure 6). A constant level of noise can easily affect the smaller peak (^{22}Ne) relatively more, possibly causing a bias in the determination of the ^{22}Ne/^{20}Ne ratio in air. The routine used to determine the peak heights, described in the QMS Analysis section, was carefully designed to avoid this sort of bias as much as possible. In contrast, a systematic bias that equally affected all our determinations of the MFF would cancel out of the final calculations, because a mass fractionation correction is applied to both the reverse isotope dilution calculation, to determine the spike concentration, and the normal isotope dilution calculation, to determine the sample concentration (Poole et al., 1997). However, it was still necessary to precisely account for changes in the MFF, because spike calibrations were done only at widely spaced intervals, and the MFF can drift a couple of percent over several months. The difference between the precisions calculated from duplicates and from deep water intercomparisons (0.12% vs. 0.20%) may indicate some remaining bias in the peak height determinations of air samples.

To assess accuracy, we examined the possible sources of systematic offsets in the method (Table 3). Four of the possible inaccuracies considered could have had an effect of $\geq$ 0.05% on the final Ne concentrations.

First, the most recent estimate of the Ne concentration of dry air is 18.18 $\pm$ 0.04 ppm (Glueckauf, 1951). Air was the ultimate standard in calibrating the spike concentration, and the uncertainty in the air value results in a 0.2% uncertainty in the accuracy of our Ne measurements. However, this error cancels when Ne saturation is calculated, because the equilibrium concentration of Ne in water is also determined relative to the amount in air (Weiss, 1971; Top et al., 1987; Hamme and Emerson, 2004).

Second, the pressure gauge used to determine the amount of spike added to the sample flasks was factory calibrated to $\pm$0.15%. Tests on older model capacitance diaphragm gauges suggest that calibration drift rates may be well over 0.15% over several years (Hyland and Tilford, 1985), but we detected no discernable drift in the calibrations of our two gauges relative to each other. Error in the pressure reading while adding the spike produces an error of the same magnitude in the Ne concentration of the sample, and we assess this uncertainty at 0.15% based on the manufacturer specifications.

Table 3: Magnitudes of the possible systematic offsets in the method

Possible source of error	Nominal size and error	Effect on Ne conc. (%)
Ne concentration of dry air	18.18 $\pm$ 0.04 ppm	0.2
Baratron pressure gauge	600 $\pm$ 0.9 Pa	0.15
Spike concentration	11.291 $\pm$ 0.008 ppm	0.06
	10.766 $\pm$ 0.005 ppm	0.05
Sample preservation	—	0.05?
^{22}Ne abundance in spike	98.74 $\pm$ 0.14%	0.04
	99.70 $\pm$ 0.04%	0.01
Flask volume	160 $\pm$ 0.06 ml	0.04
Sample mass	200 $\pm$ 0.02g	0.02
Thermometer calibration	21 $\pm$ 0.05 °C	0.01
Equilibrium fractionation of Ne between air and water	1.4 $\pm$ 0.3‰	0.01
Equilibrium fractionation of Ne between headspace and sample	0.01‰	0.001
non-ideality of gas in spike addition	—	0.0002
	—	0.0002
natural ^{22}Ne/^{20}Ne ratio	0.1020 $\pm$ 0.0008	None

Third, two separate spikes (mixtures of ^{22}Ne with N_2) have been used over several years of sample measurement. Each of the spikes was calibrated multiple times, and we found no indication that the spike had become contaminated with atmospheric Ne or that its concentration had drifted with time. The relative standard deviation of the mean for the multiple spike calibrations was 0.05–0.06%, which transfers to a 0.05–0.06% possible offset in the Ne concentrations of the samples. Inaccuracies caused by the pressure gauge cancel in the calculation of the spike calibration, hence the pressure gauge was not an additional factor in the spike concentration error.

Finally, some error must be present due to Ne leaking into or out of the samples during preservation. This variability in preservation must be small based on the excellent precision of the measurement ($\pm$0.13%). An average leak-induced error cannot be calculated from the preservation test on evacuated flasks, because the gradient across the O-rings changes significantly when spike or sample is placed in the flask. However, given that evacuated flask tests suggested a 0.1% error from leaks and that tests with flasks containing spike showed a lower
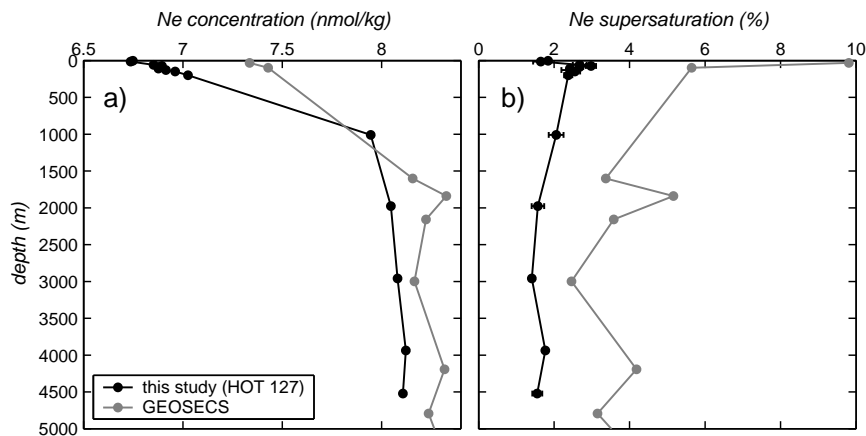
Figure 7: (a) The black line is the mean profile of Ne concentration in nmol/kg (10^{-9} mol/kg) measured in June 2001 at HOT (22.8^oN 158^oW). Error bars are smaller than the size of the points. The gray line is the nearest Ne profile measured during GEOSECS (31.4^oN 150^oW) in September 1973. (b) Mean profile of Ne supersaturation for the same data in percent. Ne solubility is calculated relative to Hamme and Emerson (2004). Error bars for the HOT data reflect the standard deviation of duplicate samples.

leak rate, we guess that an error of 0.05% is appropriate for sample preservation.

Combining all the errors considered, we estimate a ±0.18% accuracy excluding the possible error in the Ne concentration of air, and ±0.27% including this error.

3.4 Method Utility and Comparison to Previous Methods

To demonstrate the utility of this analysis method, we present a recent depth profile of Ne from the Hawaii Ocean Time-series (HOT) measured by our method and one from a nearby station measured during GEOSECS (Figure 7). The increased precision of our method is evident from the lower variability in Ne concentrations, especially in deep waters. The offset between our data and GEOSECS could indicate air contamination or calibration problems with the GEOSECS data. Typical Ne concentrations measured in the open ocean range from 6.7 to 8.2 nmol/kg. Trends in concentration are controlled mainly by temperature. When the measured concentrations were compared to the equilibrium Ne concentrations expected for the potential temperature and salinity of the water (Hamme and Emerson, 2004), Ne was found to be 1.5–3% supersaturated throughout the water column. The small subsurface peak in supersaturation, centred at 75 m, is caused by warming of this water mass, which is within the euphotic zone but beneath the mixed layer in June (Well and Roether, 2003).

This method differs from other published Ne analysis methods mainly in its procedure for sample collection. The copper tube sampling method offers the advantage of excellent long-term preservation of the samples until analysis. However, the glass flask sampling method described here, featuring the use of CO_2 to flush air from the flask neck before sampling, greatly reduces the chance that small air bubbles could be trapped in the sample, causing contamination. Also, the error in determining sample weight is reduced using our glass flask method, because the weight of an empty glass flask is 10 times less than that of an empty Cu tube and holder. Finally, the use of isotope dilution eliminates the need to completely degas the sample and corrects for drift in the sensitivity of the QMS, but requires accurate determinations of mass fractionation.

The equipment required for sample collection and analysis with this method is relatively inexpensive. Currently, the total time for analysis of one sample is two hours, and

11

the process is entirely manually operated. Because the pressure gauge calibration is the method's main source of inaccuracy, we suggest that anyone wishing to duplicate this method choose a higher accuracy pressure gauge to add the spike, as better models than the one described here have become available. Meaningful improvements could also probably be made in the preservation of samples collected in glass flasks. With an additional monetary investment, automation of the analysis could be achieved, which would significantly decrease the individual attention required to run samples and perhaps increase the precision of the method. If smaller sample sizes and reduced analysis time are desired, a trap whose temperature could be reduced to 10–40 K could be used to concentrate the Ne near the inlet to the QMS (Lott and Jenkins, 1984; Lott, 2001). Reduced analysis time could also be achieved through faster analog signal conversion and data storage.

References

Bieri, R. H., 1971. Dissolved noble gases in marine waters. Earth Planet. Sci. Lett. 10 (3), 329–333.

Bieri, R. H., Koide, M., Goldberg, E. D., 1968. Noble gas contents of marine waters. Earth Planet. Sci. Lett. 4, 329–340.

Craig, H., Hayward, T., 1987. Oxygen supersaturation in the ocean: Biological versus physical contributions. Science 235 (4785), 199–202.

Craig, H., Weiss, R. F., 1971. Dissolved gas saturation anomalies and excess helium in the ocean. Earth Planet. Sci. Lett. 10 (3), 289–296.

Craig, H., Weiss, R. F., Clarke, W. B., 1967. Dissolved gases in the Equatorial and South Pacific Ocean. J. Geophys. Res. 72 (24), 6165–6181.

Eberhardt, P., Eugster, O., Marti, K., 1965. A redetermination of the isotopic composition of atmospheric neon. Z. Naturforschg. 20 a, 623–624.

Emerson, S., Quay, P. D., Stump, C., Wilbur, D., Schudlich, R., 1995. Chemical tracers of productivity and respiration in the subtropical Pacific Ocean. J. Geophys. Res. 100 (C8), 15,873–15,887.

Emerson, S., Stump, C., Wilbur, D., Quay, P., 1999. Accurate measurement of O_2, N_2, and Ar gases in water and the solubility of N_2. Mar. Chem. 64 (4), 337–347.

Glueckauf, E., 1951. The composition of atmospheric air. In: Malone, T. F. (Ed.), Compendium of Meteorology. American Meteorological Society, Boston, MA, pp. 3–10.

Hamme, R. C., 2003. Applications of neon, nitrogen, argon and oxygen to physical, chemical and biological cycles in the ocean. Ph.D. thesis, University of Washington.

Hamme, R. C., Emerson, S. R., 2002. Mechanisms controlling the global oceanic distribution of the inert gases argon, nitrogen and neon. Geophys. Res. Lett. 29 (23), 2120, doi:10.1029/2002GL015273.

Hamme, R. C., Emerson, S. R., 2004. The solubility of neon, nitrogen and argon in distilled water and seawater. Deep-Sea Res. I in press.

Hohmann, R., Schlosser, P., Jacobs, S., Ludin, A., Weppernig, R., 2002. Excess helium and neon in the southeast Pacific: Tracers for glacial meltwater. J. Geophys. Res. 107 (C11), 3198, doi:10.1029/2000JC000378.

Hood, E. M., 1998. Characterization of air-sea gas exchange processes and dissolved gas/ice interactions using noble gases. Ph.D. thesis, MIT/WHOI.

Hyland, R. W., Tilford, C. R., 1985. Zero stability and calibration results for a group of capacitance diaphram gages. J. Vac. Sci. Technol. A 3 (3), 1731–1737.

Jenkins, W. J., 1988. The use of anthropogenic tritium and helium-3 to study subtropical gyre ventilation and circulation. Philos. Trans. R. Soc. Lond., A 325 (1583), 43–61.

Kulongoski, J. T., Hilton, D. R., 2002. A quadrupole-based mass spectrometric system for the determination of noble gas abundances in fluids. Geochem. Geophys. Geosyst. 3 (6), doi:10.129/2001GC000267.

Lott, D. E., Jenkins, W. J., 1984. An automated cryogenic charcoal trap system for helium isotope mass spectrometry. Rev. Sci. Instrum. 55 (12), 1982–1988.

Lott, III, D. E., 2001. Improvements in noble gas separation methodology: A nude cryogenic trap. Geochem. Geophys. Geosyst. 2, doi:10.129/2001GC000202.

Ludin, A., Weppernig, R., Bönisch, G., Schlosser, P., 1998. Mass spectrometric measurement of helium isotopes and tritium in water samples. Tech. rep., L-DEO, Palisades.

MKS Instruments, 1998. 100-C Training and Reference Information. Process Analysis Products, Santa Clara, CA.

Poole, J. C., McNeill, G. W., Langman, S. R., Dennis, F., 1997. Analysis of noble gases in water using a quadrupole mass spectrometer in static mode. Appl. Geochem. 12, 707–714.

Rau, I., Putzka, A., 1999. Helium and neon implantation and memory observed in a quadrupole mass spectrometer. Nucl. Instrum. Methods B 155, 52–59.

Roether, W., Well, R., Putska, A., Rüth, C., 1998. Component separation of oceanic helium. J. Geophys. Res. 103 (C12), 27,931–27,946.

Roether, W., Well, R., Putska, A., Rüth, C., 2001. Correction to "Component separation of oceanic helium". J. Geophys. Res. 106 (C3), 4679.

Sano, Y., Tominaga, P., Wakita, H., 1982. Elemental and isotopic abundances of rare gases in natural gases obtained by a quadrupole mass spectrometer. Geochem. J. 16, 279–286.

Spitzer, W. S., 1989. Rates of vertical mixing, gas exchange and new production: Estimates from seasonal gas cycles in the upper ocean near Bermuda. Ph.D. thesis, MIT/WHOI.

Spitzer, W. S., Jenkins, W. J., 1989. Rates of vertical mixing, gas exchange and new production: Estimates from seasonal gas cycles in the upper ocean near Bermuda. J. Mar. Res. 47 (1), 169–196.

Stute, M., Schlosser, P., 1993. Principles and applications of the noble gas paleothermometer. In: Climate Change in Continental Isotopic Records, Geophysical Monograph 78. American Geophysical Union, Washington D.C., pp. 89–100.

Stute, M., Schlosser, P., Clark, J. F., Broecker, W. S., 1992. Paleotemperatures in the Southwestern United States derived from noble gases in ground water. Science 256 (5059), 1000–1003.

Top, Z., Eismont, W. C., Clarke, W. B., 1987. Helium isotope effect and solubility of helium and neon in distilled water and seawater. Deep-Sea Res. 34 (7), 1139–1148.

Top, Z., Martin, S., Becker, P., 1988. A laboratory study of dissolved noble gas anomaly due to ice formation. Geophys. Res. Lett. 15 (8), 796–799.

Walton, J. R., Cameron, A. E., 1966. The isotopic composition of atmospheric neon. Z. Naturforschg. 21 a, 115–119.

Weiss, R. F., 1968. Piggyback sampler for dissolved gas studies on sealed water samples. Deep-Sea Res. 15, 695–699.

Weiss, R. F., 1971. Solubility of helium and neon in water and seawater. J. Chem. Eng. Data 16 (2), 235–241.

Well, R., Roether, W., 2003. Neon distribution in South Atlantic and South Pacific waters. Deep-Sea Res. I 50 (6), 721–735.